Published in final edited form as:
Hepatology. 2013 October ; 58(4): 1296–1305. doi:10.1002/hep.26399.

Excess S-adenosylmethionine reroutes phosphatidylethanolamine towards phosphatidylcholine and triglyceride synthesis

Maite Martínez-Uña[1,7], **Marta Varela-Rey**[2,7], **Ainara Cano**[3], **Larraitz Fernández-Ares**[1], **Naiara Beraza**[2], **Igor Aurrekoetxea**[1], **Ibon Martínez-Arranz**[2], **Juan L García-Rodríguez**[2], **Xabier Buqué**[1], **Daniela Mestre**[1], **Zigmund Luka**[4], **Conrad Wagner**[4], **Cristina Alonso**[3], **Richard H Finnell**[5], **Shelly C Lu**[6], **M Luz Martínez-Chantar**[2], **Patricia Aspichueta**[1,8], and **José M Mato**[2,8]

[1]Department of Physiology, University of the Basque Country UPV/EHU, Medical School, Bilbao, Spain

[2]CIC bioGUNE, Ciberehd, Parque Tecnológico de Bizkaia, Bizkaia, Spain

[3]OWL, Derio, Bizkaia, Spain

[4]Department of Biochemistry, Vanderbilt University School of Medicine, Nashville, Tennesse

[5]Department of Nutritional Sciences, Dell Pediatric Institute, The University of Texas at Austin, Austin, Texas

[6]Division of Gastroenterology and Liver Diseases, USC Research Center for Liver Diseases, The Southern California Research Center for Alcoholic and Pancreatic Diseases & Cirrhosis, Keck School of Medicine USC, Los Angeles, California

Abstract

Methionine adenosyltransferase 1A (*MAT1A*) and glycine *N*-methyltransferase (*GNMT*) are the primary genes involved in hepatic S-adenosylmethionine (SAMe) synthesis and degradation, respectively. *Mat1a* ablation in mice induces a decrease in hepatic SAMe, activation of lipogenesis, inhibition of triglyceride (TG) release, and steatosis. *Gnmt* deficient mice, despite showing a large increase in hepatic SAMe, also develop steatosis. We hypothesized that as an adaptive response to hepatic SAMe accumulation, phosphatidylcholine (PC) synthesis via the phosphatidylethanolamine (PE) *N*-methyltransferase (PEMT) pathway is stimulated in *Gnmt*$^{-/-}$ mice. We also propose that the excess PC thus generated is catabolized leading to TG synthesis and steatosis via diglyceride (DG) generation. We observed that *Gnmt*$^{-/-}$ mice present with normal hepatic lipogenesis and increased TG release. We also observed that the flux from PE to PC is stimulated in the liver of *Gnmt*$^{-/-}$ mice and that this results in a reduction in PE content and a marked increase in DG and TG. Conversely, reduction of hepatic SAMe following the administration of a methionine deficient diet reverted the flux from PE to PC of *Gnmt*$^{-/-}$ mice to that of wild type animals and normalized DG and TG content preventing the development of steatosis. *Gnmt*$^{-/-}$ mice with an additional deletion of perilipin2, the predominant lipid droplet protein, maintain high SAMe levels, with a concurrent increased flux from PE to PC, but do not develop liver steatosis.

Correspondence: José M Mato, CIC bioGUNE, Parque Tecnológico de Bizkaia, 48160 Derio, Bizkaia, Spain. director@cicbiogune.es; Tel: +34-944-061300; Fax: +34-944-0611301.

[7]These authors contributed equally.

[8]Joint senior authors.

[*]None of the authors have conflict of interest to declare

Conclusion—These findings indicate that excess SAMe reroutes PE towards PC and TG synthesis, and lipid sequestration.

Keywords

glycine *N*-methyltransferase; lipidomics; lipid droplets; steatosis; PLIN2

Nonalcoholic fatty liver disease (NAFLD) is the most common liver disease in Western countries (1), frequently being associated with obesity, dyslipidemia and insulin resistance, a group of disorders that constitute the metabolic syndrome (2). Although these aforementioned conditions predispose the individual to develop NAFLD, our understanding of the mechanisms by which fat accumulates in the liver is not fully understood. Decreased content of S-adenosylmethionine (SAMe), the major biological methyl donor, has been linked to the development of NAFLD in different experimental models of steatosis in rodents and in humans (3). For instance, deletion of methionine adenosyltransferase 1A (*Mat1a*), the principal gene involved in hepatic SAMe biosynthesis (3), leads to a chronic reduction in liver SAMe level and to the spontaneous development of NAFLD (4). The mechanisms linking SAMe with lipid homeostasis are not obvious at first glance. However, two recent publications have shed light on this process by showing: 1) that low hepatic SAMe reduces phosphatidylcholine (PC) content, leading to SREBP-1 activation and lipogenesis (5); and 2) that low liver SAMe disrupts very low density lipoprotein (VLDL) assembly, leading to the synthesis of small, lipid-poor VLDL particles, and to a decrease in the secretion of triglycerides (TG) (6).

The anti-steatotic theory of SAMe has been challenged by the observation that deletion in mice of glycine *N*-methyltransferase (*Gnmt*), the main enzyme involved in hepatic SAMe catabolism (7), results in a marked increase in hepatic SAMe content and rapid NAFLD development (8). The $Gnmt^{-/-}$ mice show elevated serum aminotransferases at both 3 and 8 months of age. Histological examination of the livers of 3-month-old mutant mice showed steatosis and fibrosis, which were more pronounced in the livers of 8-month-old animals (8). At 8-months, $Gnmt^{-/-}$ mice also spontaneously developed multifocal hapatocellular carcinoma (8). This raises the question how SAMe can be both anti- and pro-steatotic at the same time? All mammalian cell types synthesize PC from choline and diglycerides (DG) via the CDP-choline pathway, but in hepatocytes, PC is also synthesized by the sequential methylation of phosphatidylethanolamine (PE), a reaction catalyzed by the enzyme PE *N*-methyltransferase (PEMT). This reaction consumes three molecules of SAMe for each molecule of PC being formed (9). Herein we propose that as an adaptive response to the accumulation of liver SAMe, the synthesis of PC via PEMT is accelerated in $Gnmt^{-/-}$ mice, and that the excess PC generated is rerouted towards DG and TG synthesis, and lipid sequestration (Figure 1).

Consistent with this hypothesis, our present observations indicate that the flux from PE to PC is stimulated in the liver of $Gnmt^{-/-}$ mice, and that this produces a reduction in hepatic content of PE and a marked increase in DG and TG, with only a slight increase in hepatic PC. Conversely, reduction of hepatic SAMe level by feeding a methionine deficient diet (MDD) reverted the flux from PE to PC of $Gnmt^{-/-}$ mice to that observed in wild type (WT) animals and normalized the hepatic content of DG and TG, further confirming the steatotic effect of high SAMe concentrations. Importantly, $Gnmt^{-/-}$ mice with an additional deletion of perilipin2 (*Plin2* previously known as *Adfp* or *Adrp*) (10), a gene whose expression is induced upon *Gnmt* ablation (11), maintain high SAMe levels with a concurrent increased flux from PE to PC, but fail to develop liver steatosis. *Plin2* is the predominant intracellular lipid droplet (LD) protein in hepatocytes (12), and a gene whose deletion protects against fatty liver (13).

Collectively, these findings indicate: 1) that SAMe regulates liver lipid homeostasis through a concerted collection of homeostatic actions that include: activation of lipogenesis and inhibition of TG secretion at low SAMe, and activation of TG synthesis via PEMT at high SAMe concentrations; and 2) that too much or too little SAMe can lead to an imbalance of these homeostatic actions and result in overt steatosis.

Experimental Procedures

Animals

3-month-old male *Gnmt*$^{-/-}$, *Plin2*$^{-/-}$, *Gnmt*$^{-/-}$/*Plin2*$^{-/-}$ mice and their WT litermates were produced in the animal facility of bioGUNE. They were maintained on a rodent chow diet (Teklad Global, Diet 2018S), or a MDD (S8946-E020 EF AIN 76A 0,15% L-methionine, SSNIFF, Soest, Germany) for 21 days prior to being euthanized. Animal procedures were approved by the UPV/EHU and bioGUNE Animal Care and Use Committees.

Generation of *Plin2*$^{-/-}$ and *Gnmt*$^{-/-}$/*Plin2*$^{-/-}$ mice

Subjects consisted of male and female *Plin2*$^{+/+}$, *Plin2*$^{+/-}$ and *Plin2*$^{-/-}$ mice on a mixed 129SvEv/C57BL/6J background. *Plin2 Gt(OST170322)Lex* mutant mice (derived from OmniBank ES cell line OST170322) containing a gene trap vector inserted into the first intron of the *Plin2* gene were obtained from the Texas A&M Institute for Genomic Medicine. *Gnmt*$^{-/-}$ mice were crossed to *Plin2*$^{-/-}$ mice to generate *Gnmt*$^{-/-}$/*Plin2*$^{-/-}$ mice. A detailed description of the experimental procedure to generate *Plin2*$^{-/-}$ mice is provided as supplementary information.

Radioisotope experiments

Hepatocytes were incubated with [^{3}H]acetate (20 μM,20 μCi/ml), [^{3}H]oleate (20 μM,2 μCi/ml) or [^{3}H]ethanolamine (5 μCi/ml) as described (14). At the indicated times cells and medium were separated, lipids extracted (15), separated (16), and the label incorporated into lipids determined. A detailed description of the methods is provided as supplementary information.

Ketone bodies, acid-soluble metabolites and glucose measurements

Serum ketone bodies were quantified using a kit from Wako chemicals GmbH (Richmond, VA). Acid-soluble metabolites and glucose were measured as described (17,18) and detailed in the supplementary information section.

Hepatic TG secretion rate

To measure hepatic TG secretion, mice were injected with Poloxamer P-407 (Invitrogen, Carlsbad, CA) at 1 g/kg ip as previously described (19). Prior to injection, and 2 and 6 hours after, blood samples were drawn, serum prepared, and TG concentrations determined. TG secretion rate was calculated from the difference in serum TG levels over the 6 hours following detergent injection.

Quantification of lipids

Livers (300 mg) were homogenized and lipids extracted as described (15). TG were quantified using a kit (A. Menarini diagnostics, Italy). PE, PC and DG were separated by thin layer chromatography and quantified as described (16). Microsomes were isolated from liver samples (500 mg) and lipids extracted and quantified as detailed in supplementary information.

Lipidomic analysis

Liver lipid profiles were analyzed as previously described (20). Briefly, two separate UPLC-time-of-flight (TOF)-MS based platforms analyzing methanol and chloroform/methanol liver extracts were combined. Identified ion features in the methanol extract platform included non-esterified fatty acids (FA), acyl carnitines, bile acids, monoacylglycerophospholipids, monoetherglycerophospholipids, and oxidized FA. The chloroform/methanol extract platform provided coverage over glycerolipids, cholesteryl esters, sphingolipids, diacylglycerophospholipids, and acyl-ether-glycerophospholipids. Lipid nomenclature follows the LIPID MAPS convention, www.lipidmaps.org <http://www.lipidmaps.org>.

Statistical analysis

Data are represented as means±SEM. Differences between groups were tested using the Student's t-test. Significance was defined as $p<0.05$.

Results

GNMT ablation enhances TG secretion

GNMT catalyzes the synthesis of sarcosine (methyl-glycine) from glycine, a reaction that consumes one molecule of SAMe for each molecule of sarcosine formed (7). Sarcosine has no known essential metabolic function and is demethylated, by mitochondrial sarcosine dehydrogenase, to regenerate glycine. The function of this futile cycle is to act as a cellular buffer that maintains constant the hepatic concentration of SAMe in order to avoid abnormal biological methylation reactions. Accordingly, *Gnmt* deletion results in an approximate 40-fold elevation of hepatic SAMe, and DNA hypermethylation (8). We reasoned that disruption of *Gnmt* would have no effect on hepatic lipogenesis whereas it would enhance TG secretion. To prove this hypothesis, we assayed for *de novo* synthesis of TG in hepatocytes isolated from $Gnmt^{-/-}$ mice. This was accomplished by measuring the incorporation of [^{3}H]acetate into TG (Figure 2a), and *in vivo* hepatic TG secretion following inhibition of VLDL metabolism with poloxamer (P-407) (Figure 2b). We also determined ketone bodies into serum (Figure 2c) and the *in vitro* secretion of acid-soluble metabolites (Krebs cycle metabolites and ketones) (Figure 2d), as a measure of FA β-oxidation. Whereas lipogenesis and FA β-oxidation were barely altered in hepatocytes from $Gnmt^{-/-}$ mice (Figure 2a,c,d), the hepatic TG secretion rate in GNMT-depleted livers was elevated compared to livers from WT animals (Figure 2b). Consistent with these studies, a comprehensive gene expression analysis showed that, overall, the expression of genes that supply NADPH and acyl-CoA for lipid synthesis was unaltered in mice without GNMT (Figure 2e).

Despite the marked hepatic steatosis, mice without GNMT did not show insulin resistance or changes in serum FA concentrations (Figure 1a,b, supplementary). Depletion of GNMT in mice did not alter food intake or body weight (Figure 1c,d, supplementary). The greater liver weight in $Gnmt^{-/-}$ mice was not accompanied by differences in body-weight, which may be explained by the reduced mass of the white adipose tissue in these animals (Figure 1d–f supplementary).

Gnmt ablation activates the flux from PE to PC leading to the accumulation of DG and TG

Based upon the results depicted in Figure 2, which demonstrate that $Gnmt^{-/-}$ mice have increased lipid secretion without affecting lipid synthesis or oxidation, it is not obvious how to explain the presence of fatty livers in these animals. We reasoned that an elevation of SAMe in $Gnmt^{-/-}$ mice would activate the flux from PE to PC via PEMT, which would lead to increased PC catabolism and the corresponding augmentation of hepatic DG and TG

production (Figure 2). To confirm this hypothesis, we measured the incorporation of [^{3}H]ethanolamine into PE and PC in hepatocytes isolated from 3-month old *Gnmt*$^{-/-}$ mice, and calculated the radioactivity incorporated into PC as a percentage of the radiolabel incorporated into PC+PE (Figure 3a). Because PC formed via PEMT primarily contains long-chain polyunsaturated FA (PUFA), such as docosahexaenoic acid (22:6n-3), whereas PC synthesized by the CDP-choline route do not, we also determined the PC(22:6n-3) to total PC ratio in GNMT-depleted and WT livers as a marker of hepatic PEMT activity (21). Given that PEMT activity is primarily located in the endoplasmic reticulum (22), we measured the content of PE and PC in whole liver microsomes (Figure 3b,c). As shown in Figure 3, high SAMe levels in *Gnmt*$^{-/-}$ hepatocytes associated with a 2.5-fold increase in the flux from PE to PC (p<0.001) (Figure 3a), and an increase in the PC(22:6)/PC ratio (from 0.18±0.005 in WT to 0.25±0.005 in GNMT-depleted livers, p=3.23E-06). Also as predicted, the content of PE was reduced approximately 2-fold in microsomes isolated from GNMT-depleted livers (p<0.05), whereas the amount of PC was increased 2-fold (p<0.05) (Figure 3b,c). Measurement of whole liver PE and PC content revealed a 2-fold reduction in PE (p<0.001) accompanied by a slight increase in PC (p<0.05) in the *Gnmt*$^{-/-}$ mice, as compared to WT animals (Figure 3d,e). This suggests that once translocated from the microsomes to other cellular membranes, PC is rapidly catabolized and/or secreted in high-density lipoproteins (HDL). Accordingly, loss of GNMT increased hepatic DG and TG content (Figure 4a,b), and HDL-PC levels (Figure 2a, supplementary).

Similar results were observed in 8-month old *Gnmt*$^{-/-}$ mice, indicating that PE rerouting towards PC and TG synthesis is maintained during NAFLD progression (Figure 3, supplementary).

Importantly, feeding *Gnmt*$^{-/-}$ mice a methionine deficient diet (MDD) to reduce hepatic SAMe (Table 1), reverted the flux from PE to PC to that associated with WT animals (Figure 3a), and restored normal PE, PC, DG, and TG levels (Figures 3d,e and 4a,b), preventing steatosis (Figure 2b, supplementary). In hepatocytes isolated from *Gnmt*$^{-/-}$ mice, the inhibition of PEMT with 3-deazaadenosine (DZA) (23) also resulted in decreased TG levels (Figure 4c), These data strongly support the hypothesis that hepatic lipid accumulation in the absence of GNMT is best explained by the enhanced synthesis of PC via PEMT and the catabolism of these PC to TG. Finally, we observed that the incorporation of [^{3}H]oleate into DG in hepatocytes from *Gnmt*$^{-/-}$ mice was increased 4-fold with respect to that found in WT animals (p<0.0001) and that feeding a MDD normalized [^{3}H]oleate incorporation into DG (Figure 4d). Accordingly, *Plin2*, *Cidec*, *Fitm1* and *G0s2*, which encode genes involved in lipid sequestration, and *Scd1*, a FA desaturase whose deletion protects form carbohydrate-induced steatosis (24), were upregulated in *Gnmt*$^{-/-}$ mice (Figure 4e). *Plin2, Cidec,* and *G0s2* are controlled by the pro-steatotic transcription factor PPARγ, which was among the most prominently upregulated genes in mice without GNMT (Figure 4e).

Deletion of *Plin2* in *Gnmt*$^{-/-}$ mice inhibits lipid sequestration and promotes gluconeogenesis

Increased TG and the formation of LD are the two key features of fatty liver. LD are intracellular storage places that protect neutral lipids, such as TG, DG and cholesteryl esters, from unregulated degradation (12). Upon specific stimulation, TG undergoes a cycle of lipolysis and re-esterification prior to being assembled into VLDL (25). Fatty acids are also released from LD in order to be either oxidized and generate energy, or reutilized for the synthesis of cellular membranes. Perilipin (PAT)-domain proteins form a conserved family of proteins that are localized at the surface of neutral LD. PAT-proteins not only stabilize LD, but also protect their neutral lipids from degradation (12,13). PLIN2, a member of the PAT-family, is the predominant neutral LD protein in hepatocytes (12,13). PE methylation

via PEMT has been shown to promote LD formation and stability in adipocytes and adipose tissue (26). Importantly, we previously noticed that the hepatic expression of *Plin2* was increased following *Gnmt* ablation (11). We reasoned that increased PC synthesis via PEMT would promote LD biosynthesis and steatosis in $Gnmt^{-/-}$ livers. To prove this, we created double knockout mice by crossing $Plin2^{-/-}$ mice with $Gnmt^{-/-}$ mice, to produce a novel $Gnmt^{-/-}/Plin2^{-/-}$ double knockout mouse model, in which we determined the hepatic SAMe content (Table 1) and the levels of PE and PC (Figure 5). Furthermore, we also determined the hepatic content of DG and TG (Figure 5). As shown in Table 1, *Plin2* deletion had no effect on hepatic SAMe concentration, as the double knockout mice showed a 40-fold elevation ($p<0.0001$) in SAMe which was similar to that observed in the $Gnmt^{-/-}$ animals. Consistent with this, total liver PE content was reduced 2-fold ($p<0.01$) in $Gnmt^{-/-}/Plin2^{-/-}$ mice, whereas PC levels remained normal (Figure 5a,b), suggesting that PC was rapidly catabolized just as in the $Gnmt^{-/-}$ animals. In contrast to the situation in $Gnmt^{-/-}$ mice, while DG levels in the double knockout mice were significantly elevated ($p<0.01$), the TG content actually underwent a 2-fold reduction ($p<0.05$) (Figure 5c,d). As expected, $Gnmt^{-/-}/Plin2^{-/-}$ mice failed to develop hepatic steatosis (Figure 5e) despite having high hepatic SAMe concentration (Table 1) and reduced PE levels (Figure 5). Inhibition of lipid sequestration in $Gnmt^{-/-}$ mice decreased lipogenesis, had a minor effect on secretion of acid-soluble metabolites, decreased serum ketone bodies, yet maintained a higher hepatic TG secretion rate (Figure 6a,b,c,e). The finding that the concentration of acid-soluble metabolites did not change, whereas serum ketone bodies were reduced suggests that acetyl-CoA generated via β-oxidation is driven towards the Krebs cycle and gluconeogenesis (Figure 6b,c). Accordingly, glucose production in the absence or presence of the precursors lactate/pyruvate and glycerol, was increased in hepatocytes without GNMT and PLIN2 (Figure 6d).

Identification of SAMe regulated lipids

In keeping with the lipid tracing studies, a comprehensive lipidomic analysis of livers from control diet $Gnmt^{-/-}$, MDD-treated $Gnmt^{-/-}$, and $Gnmt^{-/-}/Plin2^{-/-}$ mice was performed and compared with that of their corresponding WT animals. Increased SAMe is characterized by a marked remodeling of lipid composition (Figure 7 and Table 1 supplementary). These changes included an increase in TG that are rich in PUFA(18:2, 20:2, 20:4, 22:4, 22:5, 22:6), of DG such as DG(18:1+18:1), DG(16:0+20:4) and DG(16:0+18:1), of ceramides such as Cer(d18:1/18:0), and of free unsaturated FA (UFA)(16:1n-x, 18:1n-9, 20:3n-3 and 22:4n-6); and a marked decrease in PE rich in PUFA, and of a variety of sphingomyelins such as SM(d18:1/22:0), SM(d18:1/21:0), and SM(d17:1/22:0). We found that, after MDD treatment, $Gnmt^{-/-}$ mice revealed a lipidomic signature that resembled the signature presented by WT mice (Figure 7 and Table 1 supplementary). $Gnmt^{-/-}/Plin2^{-/-}$ mice showed also a reversal of the TG and UFA signatures, although the profile of the DG, PE and sphingomyelins in these animals resembled the lipidomic signature of $Gnmt^{-/-}$ mice, and the PC signature was only partially reverted (Figure 7, and Table 1 supplementary). These results are consistent with the observation that these double knockout mice maintain high SAMe levels with a concurrent increased flux from PE to PC, but do not develop liver steatosis.

Discussion

It has recently been suggested (27) that PC made via PEMT may be an important source of hepatic TG. Herein we investigated the role of SAMe on TG homeostasis and found that activation of PEMT by an excess of hepatic SAMe leads to increased TG synthesis and ultimately to liver steatosis. For these studies we used $Gnmt^{-/-}$ mice, a model we developed which is characterized by the high hepatic content of SAMe, and the rapid development of

fatty liver (8). We initially observed that hepatocytes from *Gnmt*$^{-/-}$ animals maintained on a normal diet present with normal lipogenesis and FA β-oxidation but with increased TG secretion. This is consistent with recent observations showing that low SAMe stimulates *de novo* lipogenesis in the liver (5), while impairing VLDL assembly and TG secretion (6). We subsequently observed that the flux from PE to PC via PEMT was markedly stimulated in *Gnmt*$^{-/-}$ hepatocytes, which is in perfect agreement with the observation that this model is characterized by a 40-fold increase in hepatic SAMe concentration. Concurrent with PEMT's cellular localization (22), we observed a reduction in microsomal PE concomitant with an increase in PC in the *Gnmt*$^{-/-}$ mice. Whereas the mass of PE in whole liver was reduced 2-fold, PC content was only slightly increased, suggesting an increase in PC catabolism and/or secretion in HDL in mutant mice. Accordingly, both the mass of hepatic DG and TG, and the serum HDL-PC levels increased in *Gnmt*$^{-/-}$ mice compared to WT animals. These results are consistent with recent findings showing that membrane PC can be an important precursor of liver TG under normal physiological conditions (28).

Administration of a MDD to *Gnmt*$^{-/-}$ mice normalized hepatic SAMe content, which is fully consistent with our understanding of the function of GNMT in methionine catabolism (7). More importantly, in addition to lowering hepatic SAMe, placing the *Gnmt*$^{-/-}$ mice on a MDD also served to restore normal hepatic lipid metabolism, indicating that SAMe is the rate-limiting substrate linking PE with TG via PC and DG. The observation that PEMT inhibition with DZA in Gnmt−/− hepatocytes resulted in decreased TG levels further supports the role of PEMT in this process. These results demonstrate for the first time that PEMT is an unexpected source of hepatic TG, particularly in cases of SAMe excess. We conclude that stimulation of the PEMT pathway induced by high SAMe can explain hepatic steatosis in *Gnmt* mutant mice. This finding is clearly relevant to human disease, as children with *GNMT* mutations were recently identified to suffer from liver injury (29,30). Although it is not yet known if PC made via PEMT is quantitatively an important source of hepatic TG under normal physiological conditions, there are situations other than *Gnmt* deletion that can augment hepatic SAMe content, such as an increase of dietary methionine (31) or cystathionine β-synthase (CBS) ablation (3). Interestingly, *Cbs*−/− mice exhibit severe liver injury, steatosis and fibrosis (32).

In a similar manner, we also investigated the role of PLIN2 on a background of high SAMe. For these studies we generated a novel, double *Gnmt*$^{-/-}$/*Plin2*$^{-/-}$ knockout mouse model that is characterized by high hepatic SAMe and low PE content, much like *Gnmt*$^{-/-}$ mice, that in contrast did not develop fatty liver. Consistent with previous findings (12,13), knockout of *Plin2* in GNMT-depleted livers decreased lipogenesis and increased TG secretion. *Plin2* ablation increased gluconeogenesis, indicating that crosstalk exists between lipid synthesis and sequestration and glucose metabolism. Since PE methylation has been shown to promote LD formation (26), these results support a model where increased PEMT activity induces both TG synthesis and its accumulation into newly formed LD.

Collectively, these observations, taken in light of previous findings (5,6), demonstrate that SAMe regulates liver lipid homeostasis through a concerted series of homeostatic actions that include: activation of lipogenesis and inhibition of TG secretion at low SAMe, and activation of TG synthesis via PEMT at high SAMe. This cascade of events goes a long way towards explaining why a chronic imbalance in hepatic SAMe synthesis (4) or catabolism (8), is capable of inducing NAFLD.

Supplementary Material

Refer to Web version on PubMed Central for supplementary material.

Acknowledgments

Virginia Gutiérrez de Juan and Begoña Rodríguez-Iruretagoyena for technical support. Azucena Castro, for discussion. Human and technical support from Unidad de formación e investigación UFI11/20, University of Basque Country.

Abbreviations used

Cer	ceramides
DG	diglycerides
DZA	3-deazaadenosine
FA	fatty acids
GNMT	glycine *N*-methyltransferase
LD	lipid droplets
MAT	methionine adenosyltransferase
MAT1A	methionine adenosyltransferase 1A
MDD	methionine deficient diet
NAFLD	nonalcoholic fatty liver disease
PAT	perilipin
PC	phosphatidylcholine
PE	phosphatidylethanolamine
PEMT	phosphatidylethanolamine *N*-methyltransferase
PLIN2	perilipin2
PUFA	polyunsaturated fatty acids
SAMe	S-adenosylmethionine
SM	sphingomyelins
TG	triglycerides
TLC	thin layer chromatography
UFA	unsaturated fatty acids
VLDL	very low density lipoprotein
WT	wild type.

References

1. Vernon G, Baranova A, Younossi ZM. Systematic review: the epidemiology and natural history of non-alcoholic fatty liver disease and non-alcoholic steatohepatitis in adults. Aliment Pharmacol Ther. 2011; 34:274–285. [PubMed: 21623852]
2. Yilmaz Y. NAFLD in the absence of metabolic syndrome: different epidemiology, pathogenetic mechanisms, risk factors for disease progression? Semin Liver Dis. 2012; 32:14–21. [PubMed: 22418884]
3. Lu SC, Mato JM. S-adenosylmethionine in liver health, injury and cancer. Physiol Rev. 2012; 92:1515–1542. [PubMed: 23073625]

4. Lu SC, Alvarez L, Huang ZZ, Chen L, An W, Corrales FJ, et al. Methionine adenosyltransferase 1A knockout mice are predisposed to liver injury and exhibit increased expression of genes involved in proliferation. Proc Natl Acad Sci USA. 2001; 98:5560–5565. [PubMed: 11320206]
5. Walker AK, Jacobs RL, Watts JL, Rottiers V, Jiang K, Finnegan DM, et al. A conserved SREBP-1/phosphatidylcholine feedback circuit regulates lipogenesis in metazoans. Cell. 2011; 147:840–852. [PubMed: 22035958]
6. Cano A, Buqué X, Martínez-Uña M, Aurrekoetxea I, Menor A, García-Rodríguez JL, et al. Methionine adenosyltransferase 1A gene deletion disrupts hepatic very low-density lipoprotein assembly in mice. Hepatology. 2011; 54:1975–1986. [PubMed: 21837751]
7. Luka Z, Mudd SH, Wagner C. Glycine N-methyltransferase and regulation of S-adenosylmethionine levels. J Biol Chem. 2009; 284:22507–22511. [PubMed: 19483083]
8. Martínez-Chantar ML, Vázquez-Chantada M, Ariz U, Martínez N, Varela M, Luka Z, et al. Loss of the glycine N-methyltransferase gene leads to steatosis and hepatocellular carcinoma in mice. Hepatology. 2008; 47(4):1191–1199. [PubMed: 18318442]
9. Mato JM, Alemany S. What is the function of phospholipid N-methylation? Biochem J. 1983; 213:1–10. [PubMed: 6311156]
10. Kimmel AR, Brasaemle DL, McAndrews-Hill M, Sztalryd C, Londos C. Adoption of PERILIPIN as a unifying nomenclature for the mammalian PAT-family of intracellular lipid storage droplet proteins. J Lipid Res. 2010; 51:468–471. [PubMed: 19638644]
11. Varela-Rey M, Martínez-López N, Fernández-Ramos D, Embade N, Calvisi DF, Woodhoo A, et al. Fatty liver and fibrosis in glycine N-methyltransferase knockout mice is prevented by nicotinamide. Hepatology. 2010; 52:105–114. [PubMed: 20578266]
12. Chang BH, Chan L. Regulation of Triglyceride Metabolism. III. Emerging role of lipid droplet protein ADFP in health and disease. Am J Physiol Gastrointest Liver Physiol. 2007; 292:G1465–G1468. [PubMed: 17194897]
13. Chang BH, Li L, Saha P, Chan L. Absence of adipose differentiation related protein upregulates hepatic VLDL secretion, relieves hepatosteatosis, and improves whole body insulin resistance in leptin-deficient mice. J Lipid Res. 2010; 51:2132–2142. [PubMed: 20424269]
14. Aspichueta P, Pérez S, Ochoa B, Fresnedo O. Endotoxin promotes preferential periportal upregulation of VLDL secretion in the rat liver. J Lipid Res. 2005; 46:1017–1026. [PubMed: 15716580]
15. Bligh EG, Dyer WJ. A rapid method of total lipid extraction and purification. Can J Biochem Physiol. 1959; 37:911–917. [PubMed: 13671378]
16. Ruiz JI, Ochoa B. Quantification in the subnanomolar range of phospholipids and neutral lipids by monodimensional thin-layer chromatography and image analysis. J Lipid Res. 1997; 38:1482–1489. [PubMed: 9254073]
17. Cole LK, Jacobs RL, Vance DE. Tamoxifen induces triacylglycerol accumulation in the mouse liver by activation of fatty acid synthesis. Hepatology. 2010; 52:1258–1265. [PubMed: 20658461]
18. Sun Z, Miller RA, Patel RT, Chen J, Dhir R, Wang H, et al. Hepatic Hdac3 promotes gluconeogenesis by repressing lipid synthesis and sequestration. Nature Med. 2012; 18:934–942. [PubMed: 22561686]
18. Millar JS, Cromley DA, McCoy MG, Rader DJ, Billheimer JT. Determining hepatic triglyceride production in mice: comparison of poloxamer 407 with Triton WR-1339. J Lipid Res. 2005; 46:2023–2028. [PubMed: 15995182]
20. Barr J, Caballería J, Martínez-Arranz I, Domínguez-Díez A, Alonso C, Muntané J, et al. Obesity-dependent metabolic signatures associated with nonalcoholic fatty liver disease progression. J Prot Res. 2012; 11:2521–2532.
21. Watkins SM, Zhu X, Zeisel SH. Phosphatidylethanolamine-*N*-methyltransferase activity and dietary choline regulate liver-plasma lipid flux and essential fatty acid metabolism in mice. J Nutr. 2003; 133:3386–3391. [PubMed: 14608048]
22. Cui Z, Vance JE, Chen MH, Voelker DR, Vance DE. Cloning and expression of a novel phosphatidylethanolamine N-methyltransferase. A specific biochemical and cytological marker for a unique membrane fraction in rat liver. J Biol Chem. 1993; 268:16655–16663. [PubMed: 8344945]

23. Samborski RW, Ridgway ND, Vance DE. Metabolism of molecular species of phosphatidylethanolamine and phosphatidylcholine in rat hepatocytes during prolonged inhibition of phosphatidylethanolamine N-methyltransferase. J Lipid Res. 1993; 34:125–137. [PubMed: 8445336]
24. Miyazaki, et al. Hepatic stearoyl-CoA desaturase-1-deficiency protects from carbohydrate-induced adiposity and hepatic steatosis. Cell Metab. 2007; 6:484–496. [PubMed: 18054317]
25. Wiggins D, Gibbons GF. The lipolysis/esterification cycle of hepatic triacylglycerol. Its role in the secretion of very-low-density lipoprotein and its response to hormones and sulphonylureas. Biochem J. 1992; 284:457–462. [PubMed: 1599431]
26. Hörl G, Wagner A, Cole LK, Malli R, Reicher H, Kotzbeck P, et al. Sequential synthesis and methylation of phosphatidylethanolamine promote lipid droplet biosynthesis and stability in tissue culture and in vivo. J Biol Chem. 2011; 286:17338–17350. [PubMed: 21454708]
27. Vance DE. Physiological roles of phosphatidylethanolamine *N*-methyltransferase. Biochim Biophys Acta. 2013; 1831:626–632. [PubMed: 22877991]
28. van der Veen JN, Lingrell S, Vance DE. The membrane lipid phosphatidylcholine is an unexpected source of triacylglycerol in the liver. J Biol Chem. 2012; 287:23418–23426. [PubMed: 22610093]
29. Mudd SH, Cerone R, Schiaffino MC, Fantasia AR, Minniti G, Caruso U, et al. Glycine N-methyltransferase deficiency: a novel inborn error causing persistent isolated hypermethioninaemia. J Inherit Metab Dis. 2001; 24:448–464. [PubMed: 11596649]
30. Augoustides-Savvopoulou P, Luka Z, Karyda S, Stabler SP, Allen RH, Patsiaoura K, et al. Glycine *N*-methyltransferase deficiency: a new patient with a novel mutation. J Inherit Metab Dis. 2003; 26:745–759. [PubMed: 14739680]
31. Finkelstein J, Martin JJ. Methionine metabolism in mammals: adaptation to methionine excess. J Biol Chem. 1986; 261:1582–1587. [PubMed: 3080429]
32. Robert K, Nehmé J, Bourdon E, Pivert G, Friguet B, Delcayre C, et al. Cystathionine beta synthase deficiency promotes oxidative stress, fibrosis, and steatosis in mice liver. Gastroenterology. 2005; 128:1405–1415. [PubMed: 15887121]

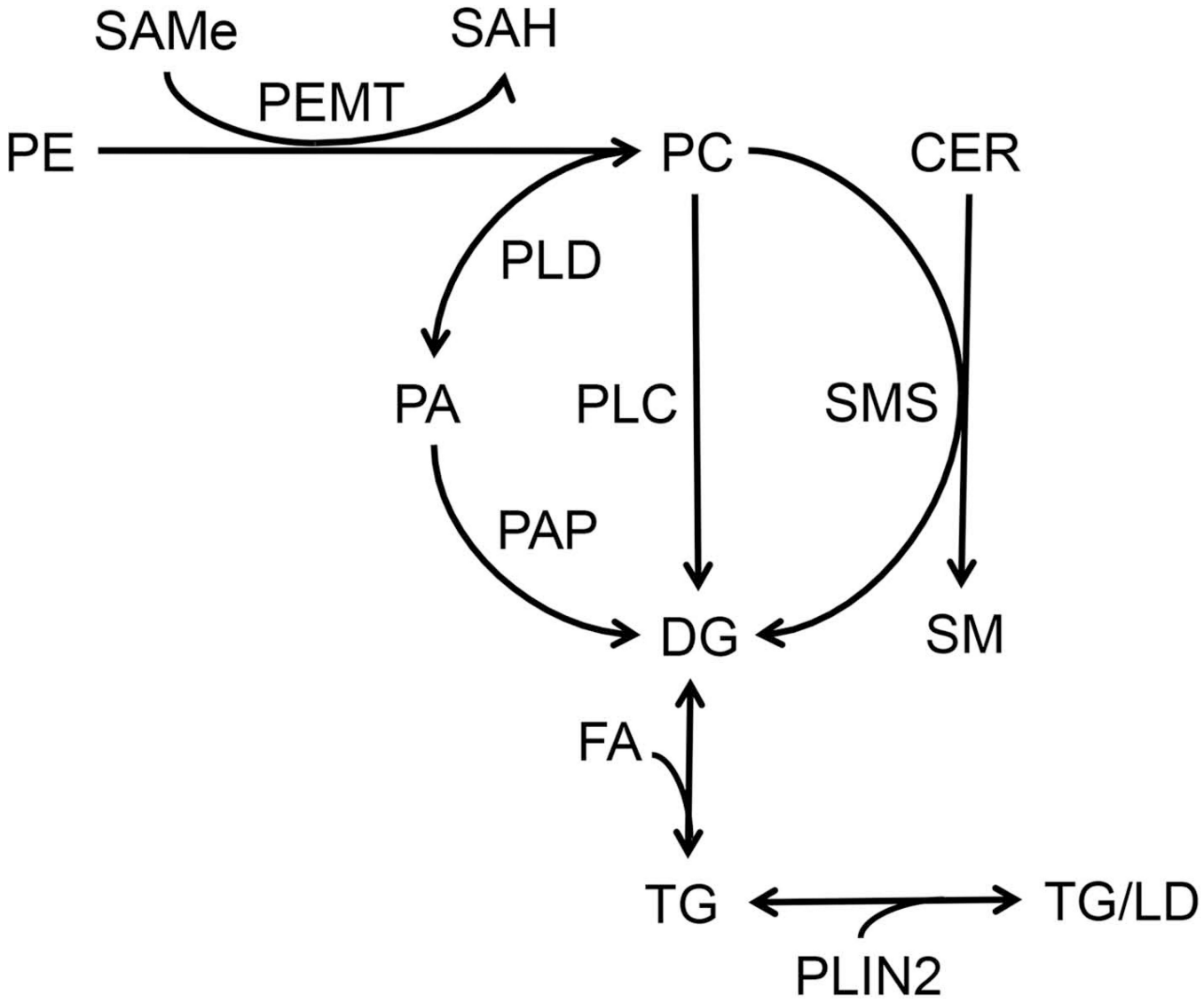

Figure 1. Schematic representation of the role of SAMe in mediating TG synthesis via PEMT

PE, phosphatidylethanolamine; PC, phosphatidylcholine; PA, phosphatidic acid; CER, ceramide; SM, sphingomyelin; DG, diglycerides; FA, fatty acids; TG, triglycerides; LD, lipid droplets; PEMT, PE *N*-methyltransferase; PLD, phospholipase D; PAP, PA phosphatase; PLC, phospholipase C; SMS, sphingomyelin synthase; PLIN2, perilipin2

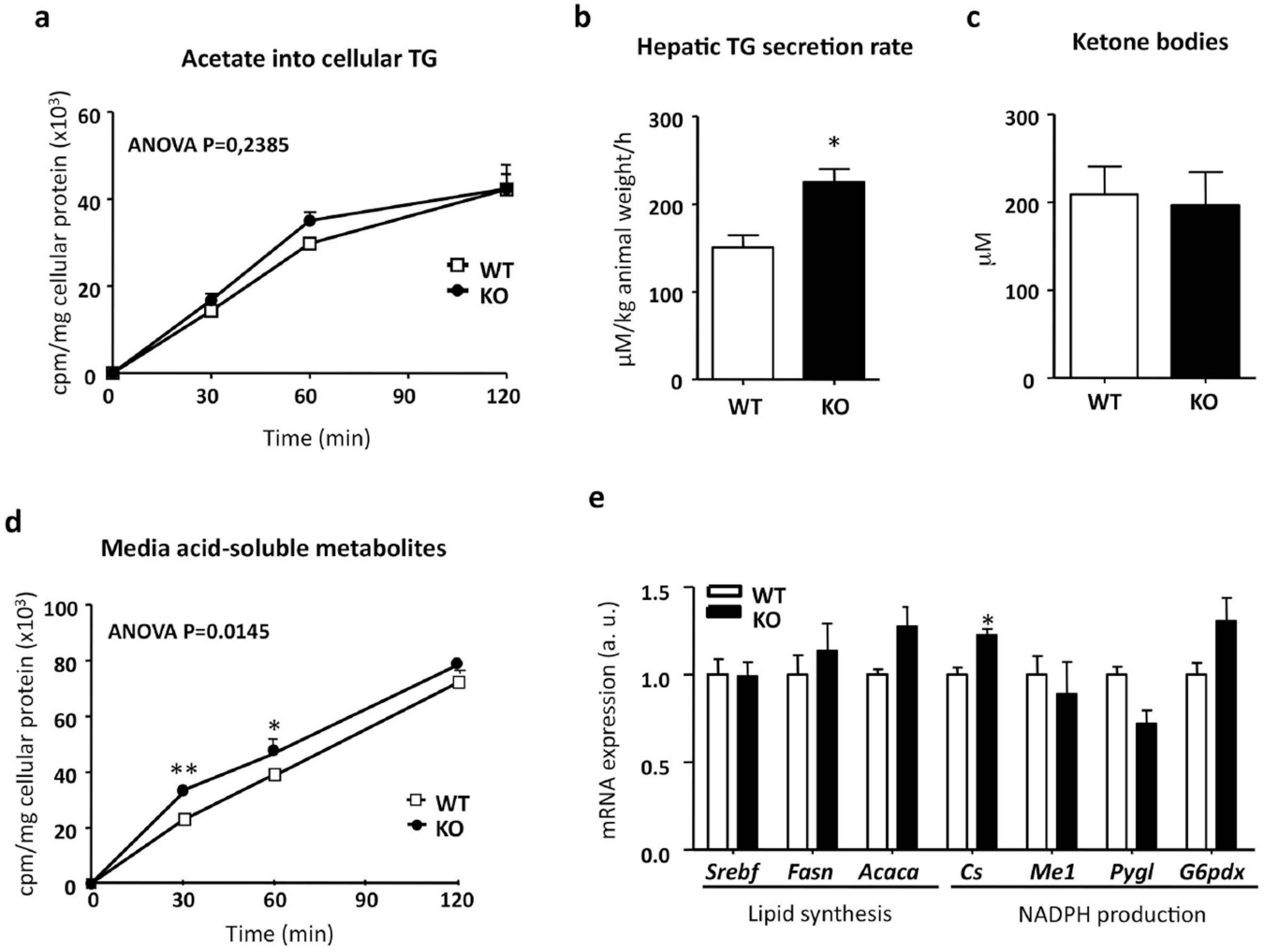

Figure 2. *Gnmt* ablation inhibits lipogenesis and enhances TG secretion

3-month-old wild type (WT) and *Gnmt*$^{-/-}$ (KO) were fasted 2 hours before experiments were performed. (a) Hepatocytes were isolated and incubated with [^{3}H]acetate for the time indicated. Radioactivity incorporated into TG was assessed with a scintillation counter. (b) Hepatic TG secretion rate was measured after inhibition of VLDL metabolism with 1 g/kg poloxamer (P-407). (c) Serum was isolated and ketone bodies were quantified. (d) Hepatocytes were incubated with [^{3}H]oleate for the time indicated, the medium was harvested and the radiolabel in acid-soluble metabolites measured. (e) Quantitative RT-PCR analysis of hepatic genes in WT and KO mice. *Acaca*, acetyl-CoA carboxylase; *Cs*, citrate synthase; *Fasn*, fatty acid synthase; *G6pdx*, glucose-6-phosphate dehydrogenase; *Me1*, malic enzyme 1; *Pygl*, glycogen phosphorylase; *Srebf*, sterol regulatory element-binding proteins. Values are means±SEM of 4–6 animals per group. Statistical differences between KO and WT mice are denoted by *p<0.05 and **p<0.01 (Student's t test) and by two-way ANOVA.

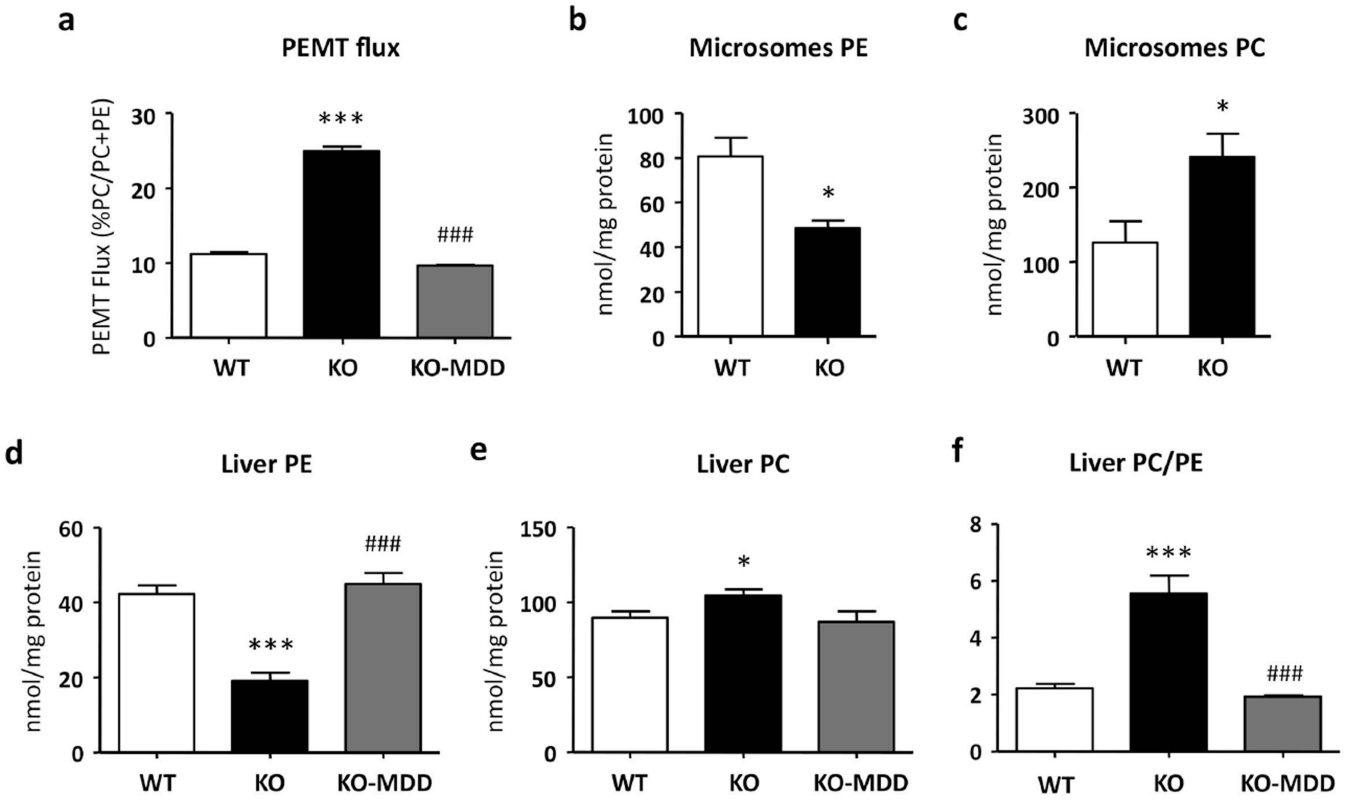

Figure 3. Restoration of normal hepatic flux from PE to PC in *Gnmt*$^{-/-}$ mice after feeding a methionine deficient diet

3-month-old wild type (WT), *Gnmt*$^{-/-}$ (KO), and *Gnmt*$^{-/-}$ mice fed a MDD (KO-MDD) for 3 weeks were fasted 2 hours before experiments were performed. (a) Hepatocytes were isolated and incubated with [^{3}H]ethanolamine for 4 hours, and the radioactivity incorporated into PC was expressed as a percentage of the radiolabel incorporated into PC plus PE. Microsomes were isolated from WT and *Gnmt*$^{-/-}$ mice liver, and PE (b) and PC (c) levels quantified after lipid extraction and separation by TLC. (d) Liver PE and (e) PC were quantified as mentioned before. (f) Liver PC/PE ratio. Values are means±SEM of 4–6 animals per group. Statistical differences between *Gnmt*$^{-/-}$ and WT mice are denoted by *p<0.05 and ***p<0.001 (Student's t test); between *Gnmt*$^{-/-}$ and *Gnmt*$^{-/-}$ fed a MDD are denoted by ### p<0.001 (Student's t test).

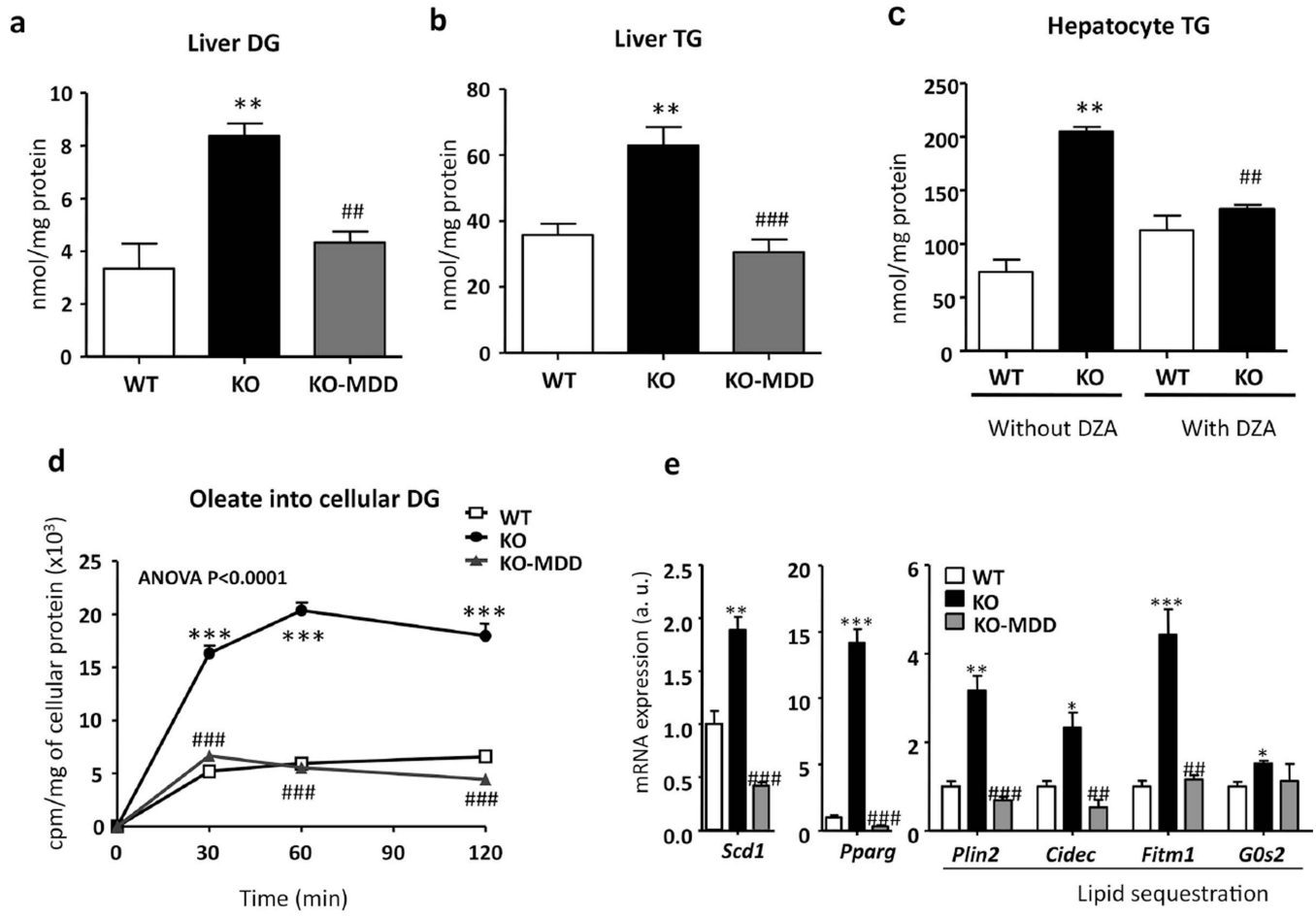

Figure 4. Restoration of normal hepatic DG and TG content in *Gnmt*$^{-/-}$ mice after feeding a methionine deficient diet

3-month-old wild type (WT), *Gnmt*$^{-/-}$ (KO), and *Gnmt*$^{-/-}$ mice fed a MDD (KO-MDD) for 3 weeks were fasted 2 hours before experiments were performed. Liver DG (a) and TG (b) were quantified after extraction and separation of lipids by TLC. (c) Hepatocytes were isolated and incubated with 3-deazaadenosine (DZA, 10 μM) for 4 hours and at the end of this period the content of TG quantified. (d) Hepatocytes were isolated and incubated with [^{3}H]oleate for the time indicated. Radioactivity incorporated into DG was assessed with a scintillation counter. (e) Quantitative RT-PCR analysis of genes in livers of WT, *Gnmt*$^{-/-}$ (KO), and MDD-treated *Gnmt*$^{-/-}$ (KO-MDD) mice. *Cidec*, cell-death-inducing DFFA-like effector c; *Fitm1*, fat storage-inducing transmembrane protein 1; *G0s2*, G0/G1 switch gene; *Plin2*, perilipin 2; *Pparg*, peroxisome proliferator-activated receptor γ; *Scd1*, stearoyl-CoA desaturase 1. Values are means±SEM of 4–6 animals per group. Statistical differences between *Gnmt*$^{-/-}$ and WT mice are denoted by **p<0.01 and ***p<0.001 (Student's t test); between *Gnmt*$^{-/-}$ and *Gnmt*$^{-/-}$ fed a MDD are denoted by ### p<0.001 (Student's t test). Multiple comparisons among groups were statistically evaluated by two-way ANOVA.

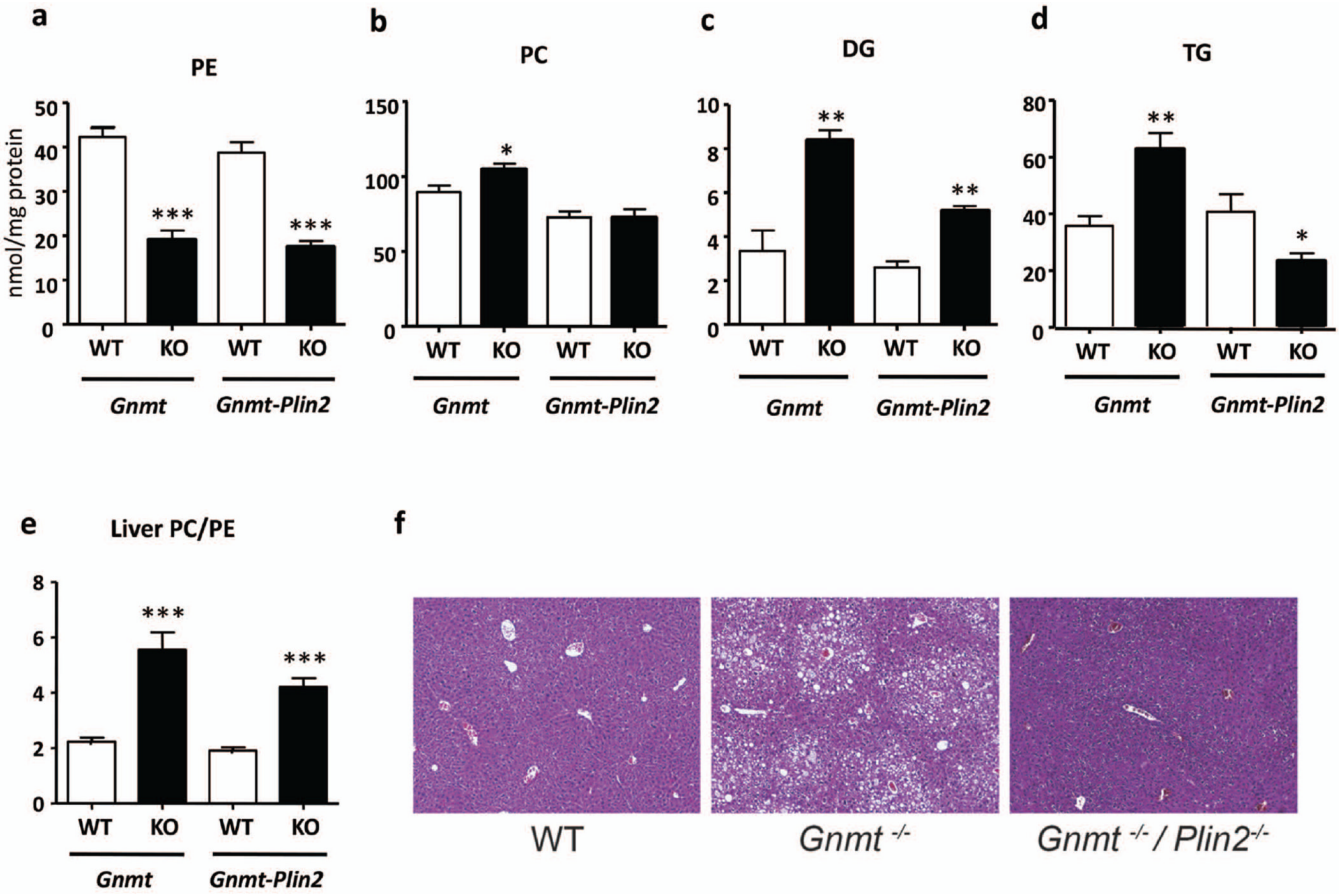

Figure 5. Deletion of PLIN2 in *Gnmt*$^{-/-}$ mice prevents liver steatosis

3-month-old *Gnmt*$^{-/-}$, *Gnmt*$^{-/-}$/*Plin2*$^{-/-}$ and their wild types (WT) were fasted 2 hours before experiments were performed. (a) PE, (b) PC, (c) DG, and (d) TG levels were quantified in liver after extraction and separation of lipids by TLC. (e) Liver PC/PE ratio. (f) Representative hematoxylin and eosin staining from 3-month-old wild type (WT), *Gnmt*$^{-/-}$ and *Gnmt*$^{-/-}$/*Plin2*$^{-/-}$ mice. Values are means±SEM of 4–6 animals per group. Statistical differences between *Gnmt*$^{-/-}$ and WT mice are denoted by *p<0.05; **p<0.01; ***p<0.001 (Student's t test).

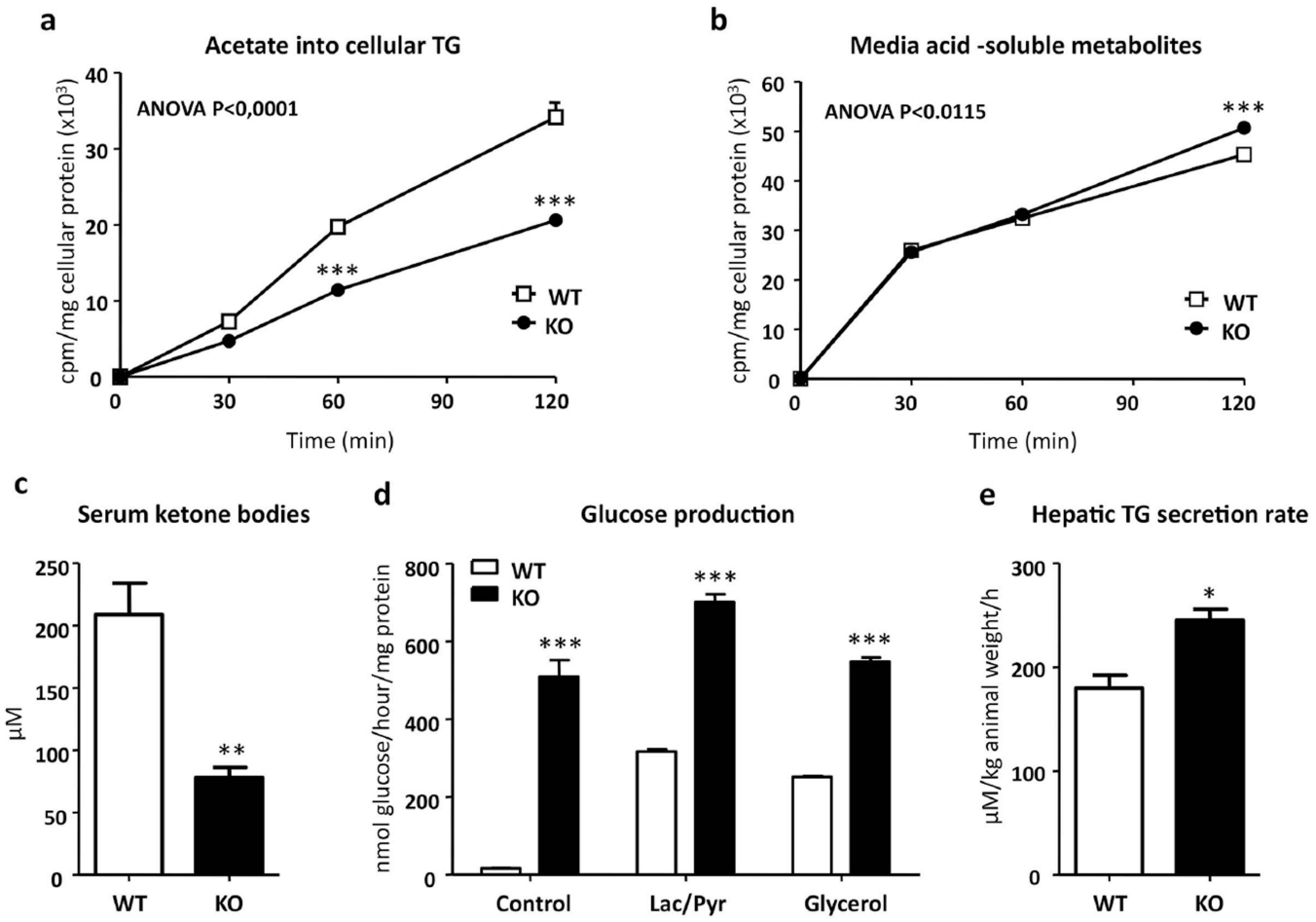

Figure 6. Deletion of *Plin2* in *Gnmt*$^{-/-}$ mice promotes gluconeogenesis

3-month-old wild type (WT) and *Gnmt*$^{-/-}$/*Plin2*$^{-/-}$ (KO) mice were fasted 2 hours before experiments were performed. (a) Hepatocytes were isolated and incubated with [^{3}H]acetate for the time indicated. Radioactivity incorporated into TG was assessed with a scintillation counter. (b) Hepatocytes were incubated with [^{3}H]oleate for the time indicated, the medium was harvested and the radiolabel in acid-soluble metabolites measured. (c) Serum was isolated and ketone bodies were quantified. (d) Hepatocytes were incubated in the absence or presence of lactate plus pyruvate (Lac/Pyr) at 30 mM/3 mM or 25 mM glycerol, and glucose production determined. (e) Hepatic TG secretion rate was measured after inhibition of VLDL metabolism with 1 g/kg poloxamer (P-407). Values are means±SEM of 4–6 animals per group. Statistical differences between KO and WT mice are denoted by *p<0.05, **p<0.01 and ***p<0.001 (Student's t test) and by two-way ANOVA.

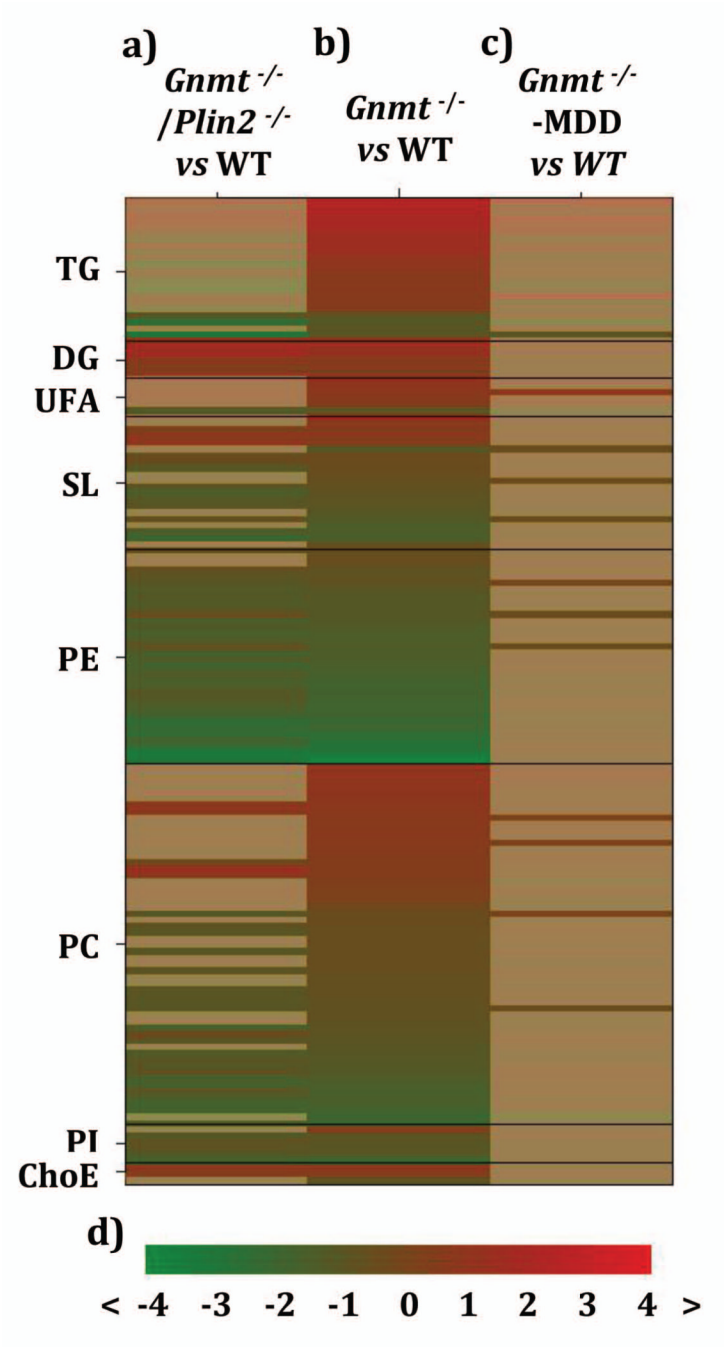

Figure 7. Identification of SAMe regulated lipids

Heat map representation of the liver lipidomic signatures obtained from *Gnmt*$^{-/-}$, MDD-treated *Gnmt*$^{-/-}$, and *Gnmt*$^{-/-}$*/Plin2*$^{-/-}$ mice. Metabolite abundance ratios in liver samples comparing (a) *Gnmt*$^{-/-}$*/Plin2*$^{-/-}$, (b) *Gnmt*$^{-/-}$, and (c) *Gnmt*$^{-/-}$-MDD with their respective WT, is shown. For each comparison, log transformed metabolite abundance ratios are depicted, as represented by the scale (d), where pronounced colours correspond to significant fold-changes (p<0.05, Student¥s or Welch's t test analysis considering 6 animals per group). Lipidomics analysis was performed as described in (20). Individual metabolite details, including fold change and statistical significance, are shown in Supplementary Table 1. TG, triglycerides; DG, diglycerides; UFA, unsaturated fatty acids; SL, sphingolipids; PE,

phosphatidylethanolamine and lysoPE; PC, phosphatidylcholines and lyso PC; PI, phosphatidylinositols and lysoPI; ChoE, cholesteryl esters.

Table 1

Hepatic SAMe content

Mouse Genotype	SAMe ± SE, pmol/mg liver tissue
WT-*Plin2*	44.7 ± 18.6
WT-*Gnmt*	65.1 ± 7.4
WT-*Gnmt* + MDD	56.4 ± 7.8
WT-*Gnmt*/WT-*Plin2*	41.7 ± 4.3
Plin2$^{-/-}$	38.7 ± 5.8
Gnmt$^{-/-}$	2,452 ± 158
Gnmt$^{-/-}$ + MDD	74.4 ± 12.6
Gnmt$^{-/-}$/*Plin2*$^{-/-}$	1,667 ± 408

The values in the table are from 3-month-old mice. Livers were collected and SAMe content determined as described (8). Data are from 4–6 animals per group. MDD, mice fed a methionine deficient diet for 3-weeks; WT, wild type mice.